JOURNAL OF APPLIED POLYMER SCIENCE VOL. 20, 367–376 (1976)

Studies on Melt Spinning. VII. Temperature Profile Within the Filament

TATSUKI MATSUO, *Katata Research Institute, Toyobo Co., Ltd., Ohtsushi, Shigaken 520-02, Japan* and
SUSUMU KASE, *Technical Exports and Licensing Division, Toyobo Co., Ltd., Kitaku Dojima, Osaka 530, Japan*

Synopsis

An attempt was made to numerically compute the temperature profile within the melt spinning filament without assuming axisymmetry and using the data on the variation of the coefficient of heat transfer from a cylinder cooled by cross flow of air as given by Eckert.[4] The computed constant-temperature contours were approximately concentric circles with their center shifted from the filament center in the downstream direction of the cooling air flow. A filament yarn melt spun under spinning conditions corresponding to the computation was dyed, and its cross sections were observed under the microscope. The border between the dyed and undyed portion of the cross sections approximately coincided with one of the computed temperature contours, suggesting indirectly the general validity of the computed temperature profile.

INTRODUCTION

Andrews[1] analyzed the temperature profile within the melt spinning filament assuming that the radius profile $R(x)$ is given and the temperature profile is axisymmetrical. However, no analytical study that appeared in the literature treats the temperature profile without assuming the axisymmetry, except one paper[2] by the present authors.

Since in most industrial melt spinning operations cooling air is blown at right angles to the filaments, one might predict the existance of a nonaxisymmetrical temperature profile across the filament. In fact, the fiber production industry sometimes takes advantage of such nonaxisymmetrical cooling in melt spinning to impart latent crimps on the melt spun fibers.[3]

In the present study, the authors numerically computed the transverse temperature profile within the filament under a representative spinning condition for PP textile filament yarn. Taken advantage of in the computation was the very convenient equivalence between the steady-state heat conduction within the melt spinning filament and the two-dimensional transient heat conduction within a stationary circular disk of fixed diameter. This equivalence introduced in an intuitive manner in the previous study[2] was derived from the basic equation of energy in the present study.

The nonaxisymmetry was introduced in the numerical computation by using the Eckert[4] data on the Nusselt number variation along the periphery of stationary cylinder cooled by a crossflow of air.

Finally, in an attempt to indirectly check the validity of the computed temperature profile, variations of dyeability over the PP filament cross sections were observed under the microscope.

DERIVATION OF GOVERNING EQUATIONS

Assuming (i) steady-state spinning, (ii) contant polymer density ρ, (iii) axisymmetrical and purely extensional flow of polymer, (iv) negligible viscous heat dissipation, and (v) negligible heat conduction in the axial direction, we may write the equations of continuity[5] and energy[6] in cylindrical coordinates for the melt spinning system shown in Figure 1 as

$$\frac{1}{r}\frac{\partial}{\partial r}(rv_r) + \frac{\partial v}{\partial x} = 0 \tag{1}$$

$$\rho C_p \left(v_r \frac{\partial t}{\partial r} + v\frac{\partial t}{\partial x}\right) = k\left\{\frac{1}{r}\frac{\partial}{\partial r}\left(r\frac{\partial t}{\partial r}\right) + \frac{1}{r^2}\frac{\partial^2 t}{\partial \theta^2}\right\} \tag{2}$$

where t is temperature, v is velocity in the x direction, C_p is specific heat, and k is heat conductivity of polymer.

At this point, we further assume that the theoretically computed filament radius profile $R(x)$ is unaffected by the existance of the radial temperature gradient. That is to say, we may separately compute $R(x)$ by solving the equations of continuity, momentum, and energy under the assumption of a flat temperature profile across the filament as was done by the authors[7] previously and, in the present analysis, use the separately computed $R(x)$ as given. This eliminates the need of the equation of momentum.

Under purely extensional flow conditions, v is independent of r, and eq. (1) becomes

$$v_r = -\frac{r}{2}\frac{dv}{dx} \tag{3}$$

showing that v_r is directly proportional to radial coordinate r. The streamline shown in Figure 1 is expressed by the equation

$$\frac{dr}{dx} = \frac{v_r}{v} = -\frac{r}{2v}\frac{dv}{dx}. \tag{4}$$

Equation (4) is readily integrated to give

$$\pi r^2 v = \text{const.} = \text{volume flow rate within radius } r. \tag{5}$$

When r above is equated to the filament radius R, we further obtain

$$\pi R^2 v = \text{const.} = \text{total volume flow rate}. \tag{6}$$

In view of eqs. (5) and (6) the quantity

$$p = \frac{r}{R(x)} \tag{7}$$

remains constant along a given stream line (see Fig. 1). In other words, a streamline can be uniquely identified by the two parameters p and θ.

Referring to Figure 1, let us consider an infinitely thin disk-like fluid ele-

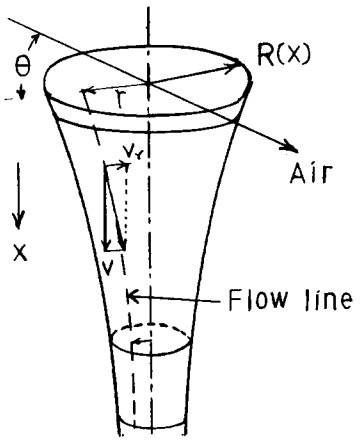

Fig. 1. Schematic of melt spinning.

ment which started to flow down the steady-state spinline at time $\tau = 0$. The location in the three-dimensional space of a point on this disk can be identified by specifying a streamline and time τ, or by giving the three parameters p, θ, and τ. In other words, the conception of the moving disk converts the independent variables in eq. (2) from (x, r, θ) to (τ, p, θ). x and r are related to τ and p, respectively, by eq. (7) above and eq. (8) below:

$$\int_0^x \frac{dx}{v(x)} = \tau. \tag{8}$$

Differentiation of temperature t with respect to τ along the streamline keeping p constant yields

$$\left(\frac{\partial t}{\partial \tau}\right)_{p=\text{const.}} = \frac{\partial t}{\partial x}\frac{dx}{d\tau} + \frac{\partial t}{\partial r}\left(\frac{\partial r}{\partial \tau}\right)_{p=\text{const.}} = \frac{\partial t}{\partial x}v + \frac{\partial t}{\partial r}v_r. \tag{9}$$

By substituting eq. (9) above into the left-hand side of eq. (2) and eq. (7) into the right-hand side of the same eq. (2), one obtains

$$\frac{R^2\rho C_p}{k}\left(\frac{\partial t}{\partial \tau}\right)_{p=\text{const.}} = \frac{1}{p}\frac{\partial}{\partial p}\left(p\frac{\partial t}{\partial p}\right) + \frac{1}{p^2}\frac{\partial^2 t}{\partial \theta^2}. \tag{10}$$

The right-hand side of eq. (10) is identical in form to that of eq. (2) since R is independent of r.

As far as the (τ, p, θ) coordinates are concerned, the restriction p = const. on the left-hand side of eq. (10) may be removed provided the partial derivatives in eq. (10) and subsequent equations are always meant to be in the (τ, p, θ) coordinates.

Substitution of eq. (8) into the left-hand side of eq. (10) yields

$$\frac{R^2\rho C_p}{k}\frac{\partial t}{\partial \tau} = \frac{R^2\rho C_p}{k}v\frac{\partial t}{\partial x}. \tag{11}$$

The $\partial t/\partial x$ in eq. (11) above is different from that in eq. (9) in that the restriction p = const. is implied.

Noting that R^2v is a constant, we further define a new variable

$$X = \frac{kx}{\rho C_p v R^2} = \frac{\pi k}{G C_p} x \tag{12}$$

where G is the mass throughput of the melt spinning. Using the new variable X, eq (10) now becomes

$$\frac{\partial t}{\partial X} = \frac{1}{p}\frac{\partial t}{\partial p} + \frac{\partial^2 t}{\partial p^2} + \frac{1}{p^2}\frac{\partial^2 t}{\partial \theta^2} \tag{13}$$

Equation (13) is the very equation of unsteady two-dimensional heat conduction, with X being the fictitious time variable. The present problem can now be treated as that of a two-dimensional transient heat conduction within a stationary disk having a fixed radius of $p = 1$.

BOUNDARY CONDITION

The boundary condition at the filament surface is

$$k\frac{\partial t}{\partial r} = (t^* - t)h \qquad \text{at } r = R \tag{14}$$

where h is the coefficient of heat transfer on the filament surface. When r is replaced with p, eq. (14) becomes

$$\frac{\partial t}{\partial p} = (t^* - t)\frac{Rh}{k} = (t^* - t)\mathrm{Nu} \tag{15}$$

where Nu is the Nusselt number.

The average of h around the filament periphery denoted here as $\bar{h}$ was expressed by the authors[7] in their previous study by an experimental formula

$$\bar{h} = 0.473\times10^{-4}\, A^{-0.667}\, G^{0.334}\, \rho^{-0.334} \times \left[1 + \left(\frac{8\rho A}{G} v_y\right)^2\right]^{0.167} \tag{16}$$

where A is the cross-sectional area of the filament and v_y is the speed of crosswise cooling air.

$R(x)$ is known, and v_y is a given spinning condition. Therefore, $\bar{h}$ can readily be calculated as a function of X using eq. (16) above.

Shown in Figure 2 is an example of the dependence of $\mathrm{Nu} = (R\bar{h}/k)$ upon X computed for the spinning condition I below.

Spinning Condition I

$t^* = 30°\mathrm{C} = \text{const.}$
$v_y = 30\ \mathrm{cm\ sec^{-1}} = \text{const.}$
$G = 0.741 \times 10^{-3}\ \mathrm{g\ sec^{-1}}$
$C_p = 0.7\ \mathrm{cal\ g^{-1}\ deg^{-1}}$ for PP
$k = 3.3 \times 10^{-4}\ \mathrm{cal\ cm^{-1}\ sec^{-1}\ deg^{-1}}$ for PP
$d_\infty = 0.6\ \mathrm{mm}$
$t_\infty = 260°\mathrm{C} =$ spinneret temperature
$v_w = 500\ \mathrm{m\ min^{-1}}$

where d_∞ is the maximum filament diameter in die swell and v_w is the take up speed. It is noteworthy that $(R\bar{h}/k)$ stays practically constant over much of the spinline except in the vicinity of the spinneret. $A(x)$ and $t(x)$ curves computed in a previous study[7] as a steady-state solution to the equations of

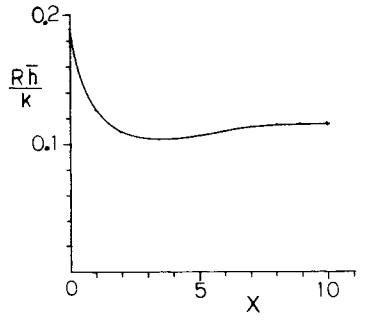

Fig. 2. Dependence of Nusselt number ($R\bar{h}/k$) on fictitious time variable X.

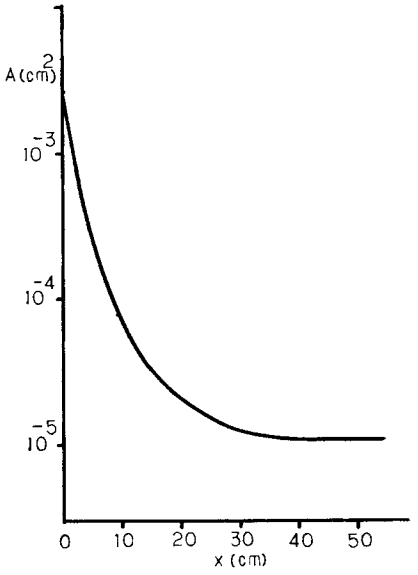

Fig. 3. Cross-sectional area profile $A(x)$ computed in a previous study.[7]

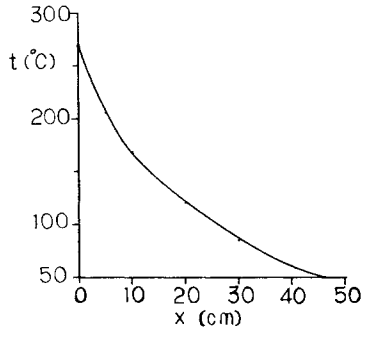

Fig. 4. Average temperature profile $t(x)$ computed in a previous study.[7]

continuity, momentum, and energy assuming a flat temperature profile across the filament and under spinning condition I above are shown in Figures 3 and 4, respectively. These $A(x)$ and $t(x)$ values were used in the above computation of ($R\bar{h}/k$).

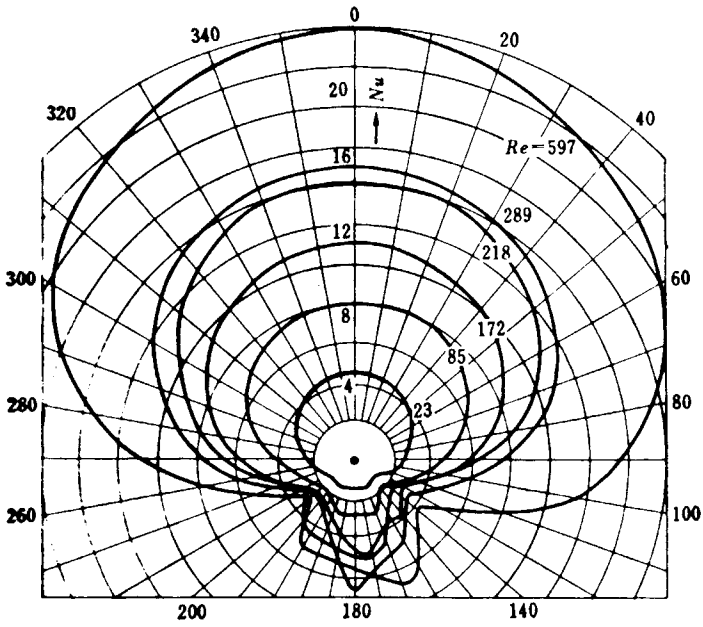

Fig. 5. Nusselt number around a stationary cylinder cooled by cross flow of air as given by Eckert.[4]

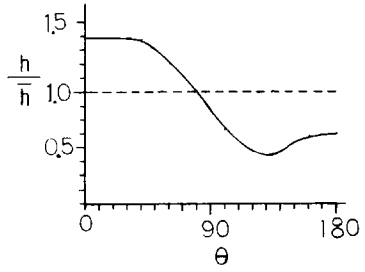

Fig. 6. Dependence of $(h/\bar{h})$ on θ used in the analysis.

Nu = Rh/k, however, is known to vary along the periphery of a stationary cylinder cooled by a cross flow of air, as the Nu-versus-θ curves under different Reynolds number Re values given by Eckert[4] show (See Fig. 5). Since the present melt spinning filament runs in the axial direction, it is not a stationary cylinder as in Eckert's experiments. However, it was simply assumed that the data shown in Figure 5 can adequately give the dependence of the ratio $(h/\bar{h})$ on θ in the present case. In the present analysis, eq. (16) was used to obtain $\bar{h}$ and the curves in Figure 5 to obtain $(h/\bar{h})$.

Considering that Re varies from about 10 to 100 along the spinline in conventional industrial melt spinning, the dependence of $(h/\bar{h})$ on θ as shown in Figure 6 was constructed out of the corresponding curves in Figure 5. The average of the $(h/\bar{h})$ curve over the filament periphery naturally is equal to unity.

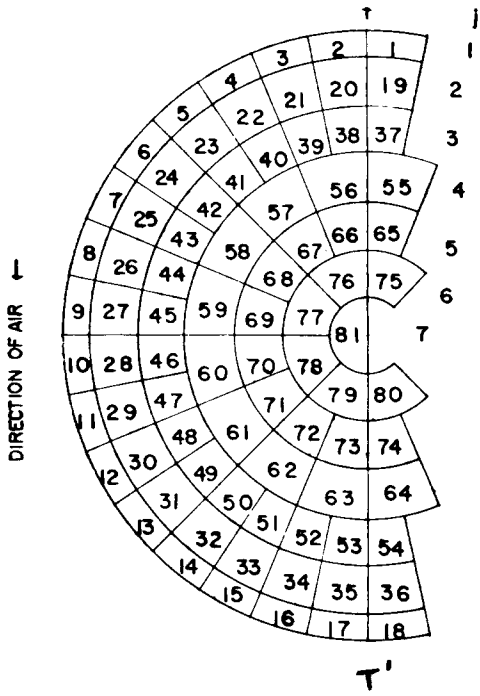

Fig. 7. Partitioning of filament cross section into 81 fictitious stirred tanks.

NUMERICAL COMPUTATION

The problem now is to solve the two-dimensional heat conduction equation, eq. (13), subject to the boundary condition, eq. (15). Direct expansion of eq. (13) into a partial difference equation gives rise to difficulty at the center of the circular filament cross section. For this reason, a direct simulation of the problem, essentially similar in principle to the finite element method, was attempted in the present study.

As shown in Figure 7, the left-hand side of the circular cross section having a unity radius was partitioned into 81 arbitrary segments. The physical interpretation of this partitioning is as follows:

(i) Each of the 81 segments is considered a stirred tank filled with liquid of uniform temperature.

(ii) The overall coefficient of heat transfer on the outmost periphery is made equal to

$$(R\bar{h}/k)(h/\bar{h}) = (Rh/k) \tag{17}$$

with the values of $(R\bar{h}/k)$ and $(h/\bar{h})$ given respectively in Figures 2 and 6 as functions of X and θ.

(iii) Since chord TT′ in Figure 7 is the direction of cooling air flow, the walls along TT′ becomes a non-conducting barrier for the reason of symmetry.

(iv) The overall coefficient of heat transfer on each wall between two adjacent stirred tanks is made equal to

k/center distance between the centers of the two stirred tanks.

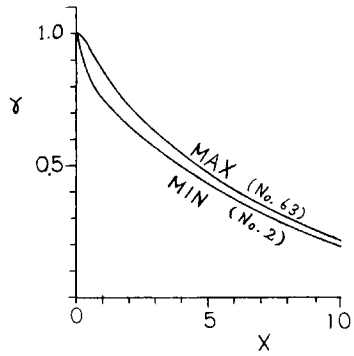

Fig. 8. Highest and lowest temperatures within the filament expressed in γ and plotted against X. Numbers are the stirred tank numbers as shown in Fig. 7.

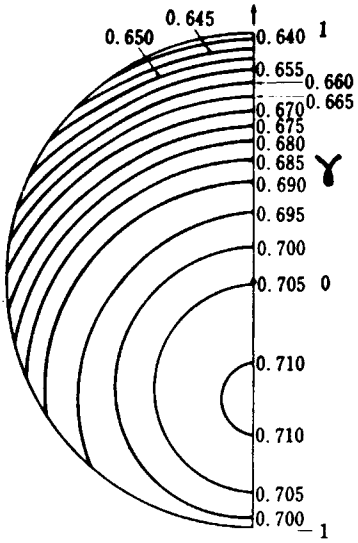

Fig. 9. Temperature contours for X = 2.0.

The proof of the validity of this simulation is not available. Since, however, the partitioning of the circle at constant radial and angular increments can be proved to be the correct differencing of eq. (13), the above simulation scheme, too, is likely to be valid.

Under the above simulation scheme, the governing difference equation for the 60th stirred tank in Figure 7 is

$$\begin{aligned} t^*_{60} = t_{60} &+ W_1(t_{59} + t_{61} - 2t_{60})\Delta X \\ &+ W_2(t_{46} + t_{47} - 2t_{60})\Delta X \\ &+ W_3(t_{70} - t_{60})\Delta X \end{aligned} \tag{18}$$

where t^*_{60} is the temperature of the 60th stirred tank for the next time increment. The governing equations for other stirred tanks are essentially similar to eq. (18) above, except for minor differences due to variations in geometrical configuration. ΔX is the difference increment in X, the dimensionless

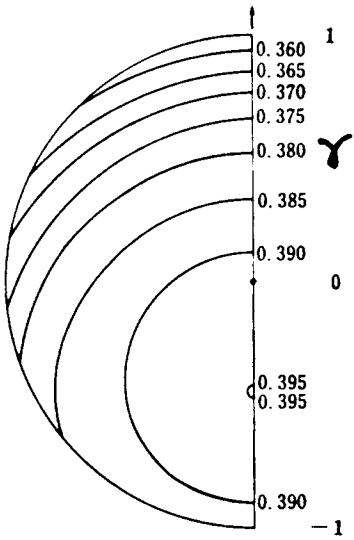

Fig. 10. Temperature contours for $X = 6.0$.

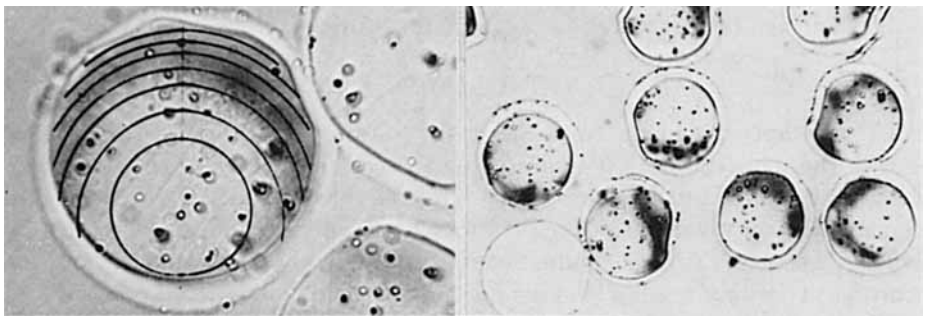

Fig. 11. Dyed and undyed portions of filament cross sections in comparison to computed temperature contours in Fig. 10.

distance from the spinneret. W_1, W_2, and W_3 are constants characterizing the geometry of the particular stirred tank.

A computer program incorporating eq. (18) and equations for other stirred tanks and having 80 FORTRAN statements was developed. When ran on an IBM-360-40 machine, the computation for spinning condition I took about 3 min under the ΔX value of 0.004.

The numerical solution for spinning condition I is summarized in Figures 8 through 10. Taking advantage of the fact that t^* in this particular case is a constant, the temperature $t(p, \theta, X)$ is expressed in a dimensionless form

$$\gamma = \frac{t - t^*}{t_\infty - t^*} \tag{19}$$

where t_∞ is the spinneret temperature (260°C). Figure 8 shows the γ-versus-X curves for the 2nd and 63rd stirred tanks which exhibited, respectively, the lowest and highest temperatures among the 81 tanks.

The temperature profiles shown in Figures 9 and 10 for dimensionless axial positions $X = 2.0$ and 6.0 are the primary results of the present study.

AN INDIRECT COMPARISON OF EXPERIMENT AND THE COMPUTED TEMPERATURE PROFILE

It is practically impossible to measure the temperature within the melt spinning filament. For this reason, an indirect verification of the computed temperature profile was attempted.

The PP filament yarn spun under spinning condition I was dyed under the following conditions:

Dye: (i) Sumiplene Bril Blue, a product of Sumitomo Chemical Co., 1% by weight of fiber; (ii) Cellion Fast Red 4 G, 2% by weight of fiber

Dispersing agent: Neugen EA-120, 2% by weight of fiber

Bath ratio: 1:50

Temperature: 100°C

Time: 1 hr

Cross sections of the dyed filament yarn observed under the microscope are shown in Figure 11. On one of the cross sections, the computed temperature profile in Figure 10 was superposed. The border between the dyed and undyed portion coincides strikingly well with one of the computed temperature contours, suggesting indirectly the general validity of the computed values. This, however, is not a conclusive proof since the relation between the dyeability and the temperature history in melt spinning is not established.

CONCLUSIONS

An attempt was made to numerically compute the temperature profile within the melt spinning filament using the coefficient of heat transfer data developed by the authors[7] previously and the dependence of Nu on angular coordinate θ as given by Eckert.[4] Proved and used in the analysis was the analogy between the heat conduction within the steady-state spinline and the transient two-dimensional heat conduction within a disk of fixed radius.

The computed temperature contours were approximately concentric, with the temperature center, or the maximum temperature point, shifted from the filament center in the direction of the cooling air flow.

A filament yarn melt spun under conditions identical to that used in the theoretical computation was dyed and observed under the microscope for filament cross sections. The border between the dyed and undyed portion of the filament cross section approximately coincided with one of the computed temperature contours, suggesting the general validity of the computed contours although not proving it conclusively.

References

1. E. H. Andrews, *Brit. J. Appl. Phys.*, **10**, 39 (1959).
2. T. Matsuo and S. Kase, *Seni Gakkai Shi* (*J. Soc. Fiber Sci. Technol. Japan*), **24**, 512 (1968).
3. T. Matsuo, S. Nanri, R. Masuda, and K. Ishitobi, U.S. Patent 3577498 (1971).
4. E. R. G. Eckert and E. Soehungen, *Trans. Amer. Soc. Mech. Eng.*, **74**, 343 (1952).
5. S. Kase and T. Matsuo, *J. Polym. Sci. A*, **3**, 2541 (1965).
6. J. M. Mckelvey, *Polymer Processing*, Wiley, New York, 1962, p. 11.
7. S. Kase and T. Matsuo, *J. Appl. Polym. Sci.*, **11**, 251 (1967).

Received January 31, 1975
Revised May 23, 1975